

# Observation of a Weak Ferromagnetic Ground State Structure for the Lithium-Insertion Compound $\text{Li}_2\text{Fe}_2(\text{MoO}_4)_3$

W. M. Reiff<sup>1</sup> and J. H. Zhang

*Department of Chemistry, Northeastern University, Boston, Massachusetts 02115*

H. Tam and J. P. Attfield<sup>1</sup>

*Department of Chemistry, University of Cambridge, Lensfield Road, Cambridge CB2 1EW, United Kingdom*

and

C. C. Torardi<sup>1</sup>

*DuPont Company, Central Research and Development, Experimental Station, Wilmington, Delaware 19880-0356*

Received August 30, 1996; in revised form February 6, 1997; accepted February 11, 1997

The low-temperature magnetism and neutron structure of orthorhombic  $\text{Li}_2\text{Fe}_2(\text{MoO}_4)_3$ , synthesized via the topotactic redox-insertion reaction of  $\text{LiI}$  with  $\text{Fe}_2(\text{MoO}_4)_3$ , is discussed. dc magnetic susceptibility measurements in an applied field of 30 G, and very low field ( $H_0 = 1$  G) ac susceptibility measurements (real and imaginary (out-of-phase) components) show a weakly ferromagnetic state, below 12.5 K, that is most likely due to intrinsic canting of antiferromagnetically coupled lattices. An analysis of the magnetic scattering from powder neutron diffraction data at 4.2 K shows an antiferromagnetic spin arrangement. Although it was not possible to refine a small magnetic component that would give rise to a net ferromagnetic moment, the magnetic space group symmetry permits a ferromagnetic component parallel to the  $x$  axis, which accounts for the weak ferromagnetism observed in the susceptibility studies. © 1997 Academic Press

## INTRODUCTION

Previously, we reported the structure and magnetism of orthorhombic  $\text{Li}_2\text{Fe}_2(\text{MoO}_4)_3$  synthesized via the topotactic, redox-insertion reaction of  $\text{LiI}$ /acetonitrile with the open-framework monoclinic compound  $\text{Fe}_2(\text{MoO}_4)_3$  (1–3). The structure, deduced from room-temperature powder X-ray and neutron diffraction measurements (1, 2), incorporates Li ions in distorted tetrahedral sites, with each  $\text{LiO}_4$  tetrahedron bridging the edges of two  $\text{FeO}_6$  octahedra (2). dc magnetic susceptibility, in applied fields as low as

30 Gauss, and zero-field Mössbauer spectroscopy measurements showed a weakly ferromagnetic state below 12.5 K that may be due to intrinsic canting of antiferromagnetically coupled lattices (1, 3). However, from a preliminary low-temperature powder neutron diffraction analysis (3), it was not possible to refine a small magnetic component that would give rise to a net ferromagnetic moment. This suggested either a field-induced canting of the spins was occurring or that a net spontaneous moment in true zero field existed, and that the spin canting necessary for this effect could not be resolved from the neutron data. We have now extended the study of the magnetism of  $\text{Li}_2\text{Fe}_2(\text{MoO}_4)_3$  by a detailed analysis of the powder neutron diffraction data and employing very low field ( $H_0 = 1$  G) ac susceptibility measurements, real and imaginary (out-of-phase) components.

## EXPERIMENTAL

### *Neutron Powder Diffraction*

The neutron powder diffraction data for  $\text{Li}_2\text{Fe}_2(\text{MoO}_4)_3$  at 4.2 K were obtained using the high-resolution five-detector diffractometer ( $\lambda = 1.546$  Å) at the National Institute for Standards and Technology as described before (2, 3). These data were analyzed by the Rietveld method using the GSAS package (4). The starting model, from the previous fit to the 300 K data (2), was refined in orthorhombic space group  $Pbcn$  using the individual profiles from the five counters. Regions of the scan corresponding to the diffraction peaks of the aluminium sample container were excluded from the analysis and the backgrounds were fitted using a refined cosine Fourier series. A good fit to the

<sup>1</sup> To whom correspondence may be addressed.

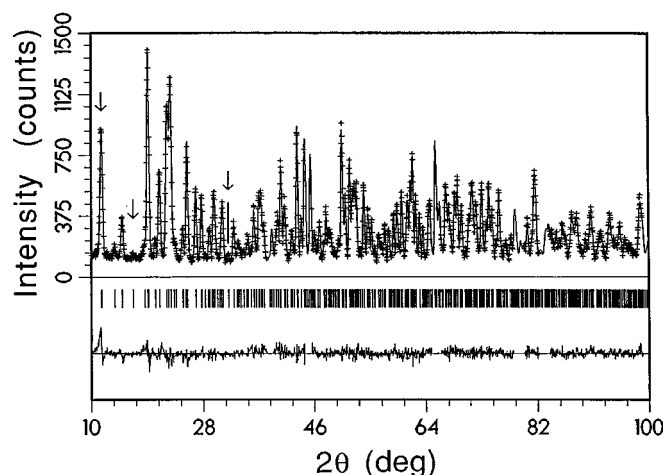


FIG. 1. Neutron powder diffraction profile and difference plots for  $\text{Li}_2\text{Fe}_2(\text{MoO}_4)_3$  at 4.2 K. Three clearly resolved magnetic peaks ((101), (201), and (203)) are marked.

nuclear peaks was obtained, and several outstanding magnetic diffraction peaks were observed at low  $2\theta$  angles (Fig. 1). The observed magnetic peaks can all be indexed on the nuclear cell and have indices  $h0l$  with  $h$  taking even and odd values, and  $l$  taking only odd values, suggesting that the magnetic moments are oriented close to the  $y$  axis, and those at sites related by the  $c$ -glide operation are antiparallel to each other. There are eight  $\text{Fe}^{2+}$  spins on one set of general equivalent positions in the unit cell, giving rise to four possible collinear antiferromagnetic models consistent with these considerations. These models were fitted to the data in turn and only one was found to fit well, with magnetic moments parallel to  $y$ , and relative spin directions as shown for the  $Y$  mode in Table 1. A projection of the magnetic structure is shown in Fig. 2.

### Magnetic Susceptibility

SQUID measurements were obtained with an S.H.E. magnetometer. ac susceptibility measurements were per-

TABLE 1  
The Relative Directions for Eight Spins Occupying One Set of General Equivalent Positions in the Three Irreducible Representations ( $X$ ,  $Y$ , and  $Z$ ) of Magnetic Symmetry Group  $Pbc'n'$

Position	$X$	$Y$	$Z$
$\pm(x, y, z)$	+	+	+
$\pm(1/2 - x, 1/2 + y, z)$	+	-	-
$\pm(x, -y, 1/2 + z)$	+	-	+
$\pm(1/2 + x, 1/2 + y, 1/2 - z)$	+	+	-

Note. The spins are parallel to the axis appropriate to each representation. The  $Y$  representation describes the observed magnetic structure of  $\text{Li}_2\text{Fe}_2(\text{MoO}_4)_3$ .

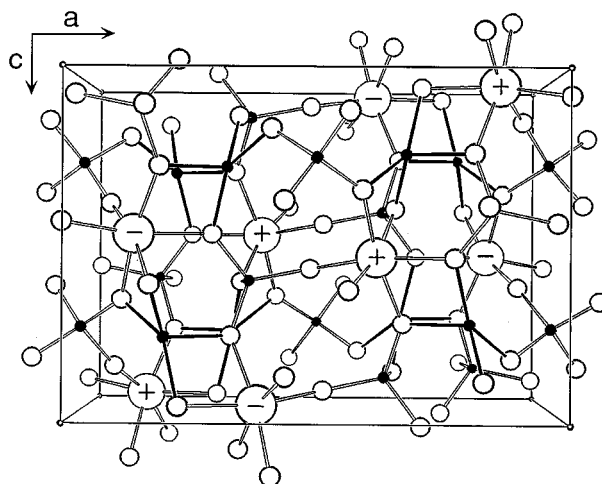


FIG. 2. A  $b$ -axis projection of the nuclear and magnetic structure of  $\text{Li}_2\text{Fe}_2(\text{MoO}_4)_3$  at 4.2 K. The directions of the electronic spins in the  $y$  direction are marked. Atomic coordinates (Tables 1 and 2) are relative to the unit-cell origin in the upper-left corner with  $+y$  oriented upward. Fe atoms are octahedrally coordinated to oxygen, Mo and Li atoms (shaded) are tetrahedrally coordinated to oxygen, and Li-O bonds are shaded.

formed at 1 Oe and 125 Hz on a Lakeshore Cryotronics Model 7000 ac susceptometer.

## RESULTS AND DISCUSSION

The observed magnetic arrangement is described by the  $Y$  irreducible representations of magnetic symmetry group  $Pbc'n'$  shown in Table 1. The other two representations, derived following Bertaut's method (5), are a ferromagnetic mode parallel to  $x$  and another antiferromagnetic mode in the  $z$  direction. Attempts to include magnetic components from these modes did not lead to any improvement in the fit. In the final refinement, both the structural and magnetic parameters were varied, giving the fit shown in Fig. 1 ( $R_{\text{WP}} = 7.2\%$ ,  $R_{\text{XP}} = 5.5\%$ , and  $\chi^2 = 1.40$ ) and the parameters in Table 2. The refined magnetic moment was  $3.91(3) \mu_{\text{B}}$  per  $\text{Fe}^{2+}$  ion. Derived bond distances and angles, which varied only slightly relative to the room-temperature structure (2), are available as supplementary tables.

No large changes are observed in the structure of  $\text{Li}_2\text{Fe}_2(\text{MoO}_4)_3$  at 4.2 K compared to that at 300 K. The  $b$ - $c$  splitting does increase upon cooling, but this does not lead to significant changes in the structure. The 4.2-K magnetic peaks are fitted by a collinear antiferromagnetic magnetic structure with moments parallel to the  $y$  axis. The observed moment of  $3.91 \mu_{\text{B}}$  (unpaired spins) is as expected for high spin  $3d^6 \text{Fe}^{2+}$ . Although the refined model is purely antiferromagnetic, the symmetry of this arrangement permits a ferromagnetic component parallel to the  $x$  axis, which accounts for the weak ferromagnetism observed in

**TABLE 2**  
The Refined Structural Parameters for  $\text{Li}_2\text{Fe}_2(\text{MoO}_4)_3$  at 4.2 K

Atom	$x$	$y$	$z$	$U_{\text{iso}} (\text{\AA}^2)$
Fe	0.3771(2)	0.2468(2)	0.4666(2)	0.0081(6)
Mo(1)	0	0.4600(4)	0.25	0.0047(11)
Mo(2)	0.3570(2)	0.4017(3)	0.1052(3)	0.0100(10)
O(1)	0.1628(3)	0.0861(4)	0.1107(4)	0.0082(11)
O(2)	0.0935(3)	0.3519(4)	0.1649(3)	0.0040(10)
O(3)	0.2809(3)	0.3299(4)	0.9660(4)	0.0102(10)
O(4)	0.4349(3)	0.0670(4)	0.3742(4)	0.0080(11)
O(5)	0.4873(3)	0.3602(4)	0.0705(4)	0.0084(9)
O(6)	0.3195(2)	0.3266(4)	0.2717(4)	0.0080(10)
Li	0.1887(9)	0.2237(15)	0.2710(13)	0.020(3)

Note. Cell parameters ( $\text{\AA}$ ):  $a = 12.8326(5)$ ,  $b = 9.4965(4)$ ,  $c = 9.2903(4)$ .

previous susceptibility measurements (1, 3). The measured magnetization at  $\sim 0.5$  kG (see Fig. 4) corresponds to a moment of  $\sim 0.3 \mu_B$  per  $\text{Fe}^{2+}$  spin, equivalent to a canting angle of  $4^\circ$  from the  $y$  axis, which is too small to be detected in the neutron experiment. Such weak ferromagnetism is often possible in antiferromagnetically ordered oxosalts with low crystal symmetry; a similar, symmetry-allowed weak ferromagnetism was found in orthorhombic  $\beta$ - $\text{CrAsO}_4$  (6), although the neutron diffraction data indicate antiferromagnetically aligned spins.

Our previous magnetic susceptibility study (1) of  $\text{Li}_2\text{Fe}_2(\text{MoO}_4)_3$  corresponds to dc Faraday balance measurements in the medium applied-field range from 1 kG to 5 kG for  $T$  varying between 1.6 K to ambient temperature. The compound exhibits weak ferromagnetic behavior via the essentially antiferromagnetic coupling ( $T_{\text{N\acute{e}el}} = 12.5$  K) of equivalent Fe(II) ions. The equivalence of the ferrous environments is confirmed by both X-ray and neutron-powder diffractometry and zero-field M\ssbauer spectroscopy. Thus, in view of the present neutron diffraction results, the observed magnetic behavior is either: (A) the result of canting induced by the applied field in our earlier dc susceptibility measurements, or (B) due to a small net moment (in zero field) owing to slight canting of the Fe(II) sublattices where the latter is simply not resolved in the present neutron diffraction study.

Essentially zero-field ac susceptibility measurements and very low field dc SQUID magnetometry are the next best approaches for us to further consider possibility (A). The lowest operating field one can reliably obtain using the SQUID magnetometry equipment available to us is  $\sim 30$  G. Such 30-G applied-field measurements are shown as  $\chi_m$ ,  $\chi_m^{-1}$ , and  $\chi_m T$  in Fig. 3. In addition, in Fig. 4, we show the field dependence of magnetization (i.e.,  $\sigma$  vs  $H_o$ ) at 6.0 K (well below  $T_{\text{N\acute{e}el}}$ ) up to  $H_o = 50$  kG with higher field resolution (initial steps of 300 G) displayed as a lower figure inset. The low-field dc susceptibility behavior is clearly similar to

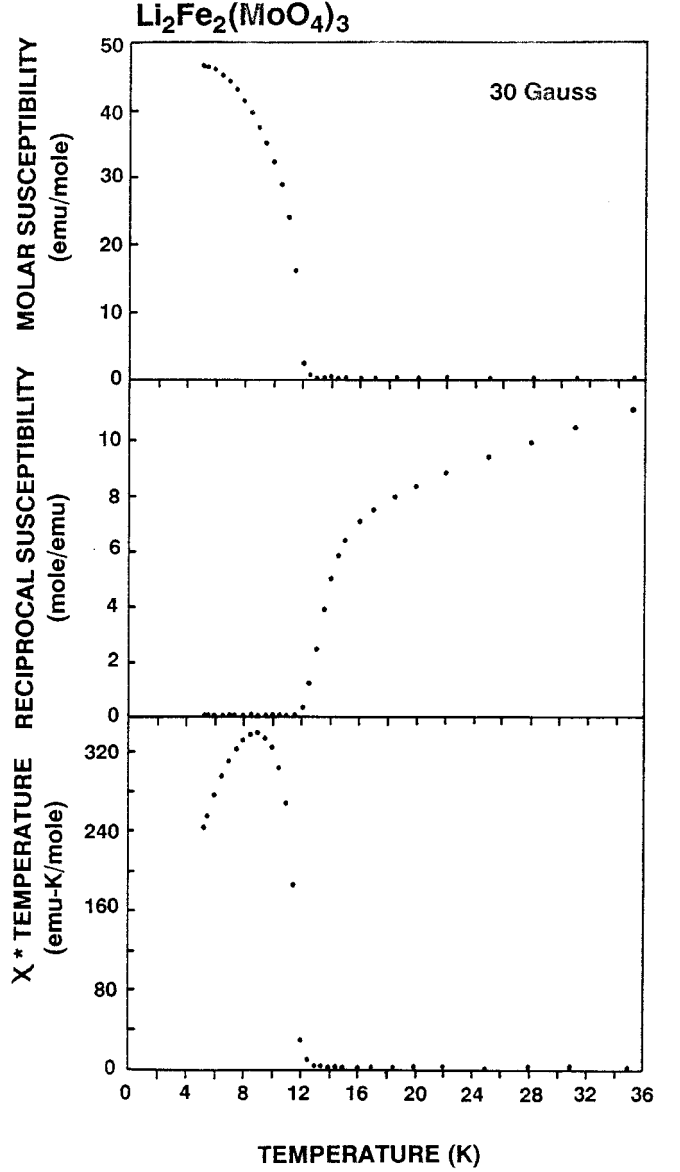


FIG. 3. SQUID magnetometry data for  $\text{Li}_2\text{Fe}_2(\text{MoO}_4)_3$  in an applied field of 30 G showing  $\chi_m$ ,  $\chi_m^{-1}$ , and  $\chi_m T$  (top to bottom).

that determined from our previous Faraday measurements. This suggests that there is likely a net spontaneous moment or magnetization in true zero field and that the spin canting necessary for spontaneous magnetization is not resolved in the neutron refinement and is, in fact, an inherent property of the system.

Within the resolution of the low-field magnetization (see Fig. 4 inset) measurements, the rapid rise in moment is typical of a ferromagnetic material. There is no evidence of sigmoidal behavior in  $\sigma$  vs  $H_o$  as, for instance, occurs in a metamagnet, wherein the applied field induces a large moment state at some critical value of  $H_o$ . Upon reaching

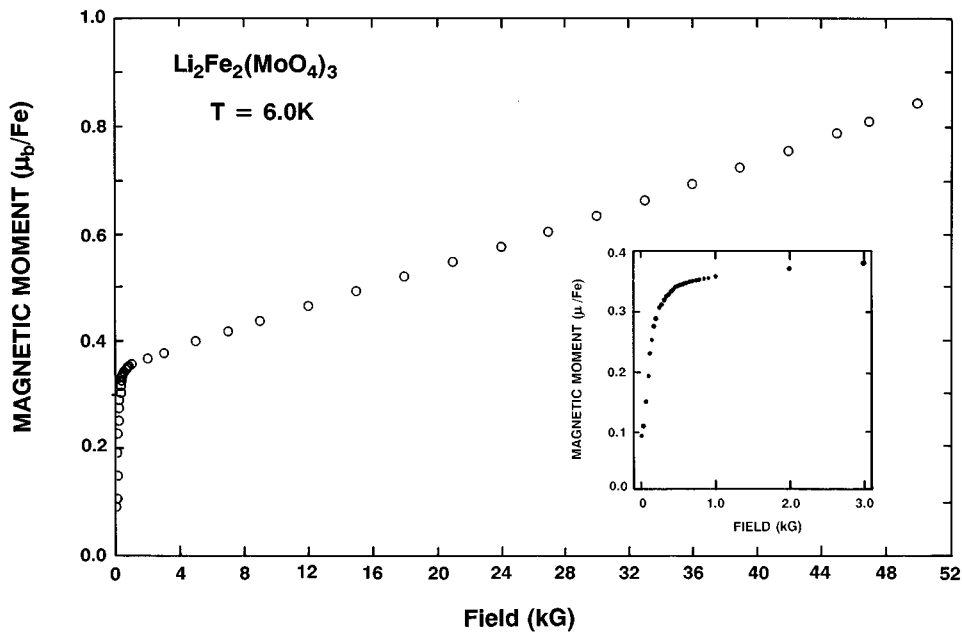


FIG. 4. Field dependence of magnetization up to 50 kG at 6 K for  $\text{Li}_2\text{Fe}_2(\text{MoO}_4)_3$ . Greater field resolution is shown in the inset.

$H_0 \sim 0.5$  kG, the value of  $\sigma$  has risen rapidly to  $\sim 0.35 \mu_B/\text{Fe}$ . However, it appears from the slope of the higher-field data, that magnetic saturation has not been reached even at  $H_0 = 50$  kG at which value  $\mu$  is approaching a value consistent with two unpaired spins per mole. This behavior is fairly typical of the orbitally anisotropic magnetic moment behavior of high-spin iron(II).

Probably the most convincing data confirming a weakly ferromagnetic ground state for  $\text{Li}_2\text{Fe}_2(\text{MoO}_4)_3$  are the ac susceptibility results ( $H_0 = 1$  Oe, 125 Hz) shown in Fig. 5 and, as a comparative check, for the precursor ferric material  $\text{Fe}_2(\text{MoO}_4)_3$ , Fig. 6. The former exhibits a rapid rise in  $\chi'_m$  below  $\sim 13$  K to a (very large) maximum of  $\sim 13$  emu/mole and an accompanying strong out-of-phase

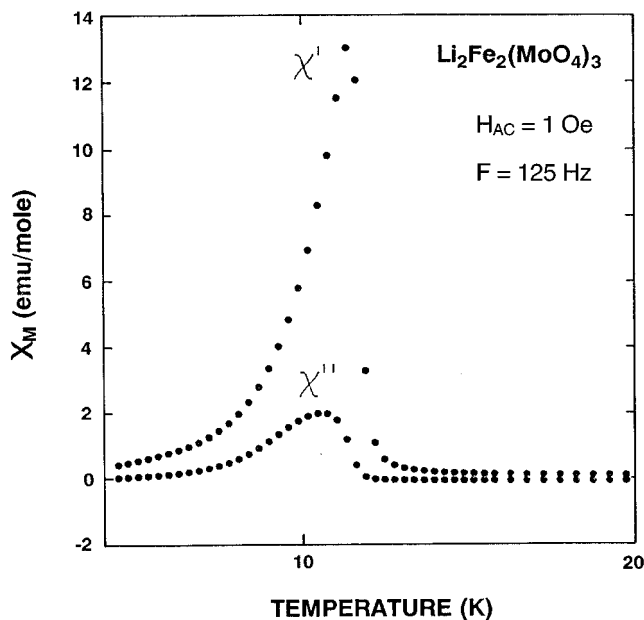


FIG. 5. Low-field ac susceptibility data for  $\text{Li}_2\text{Fe}_2(\text{MoO}_4)_3$  ( $H_0 = 1$  Oe, 125 Hz) showing a strong out-of-phase signal,  $\chi''_m$ , characteristic of a ferromagnetic ground state.

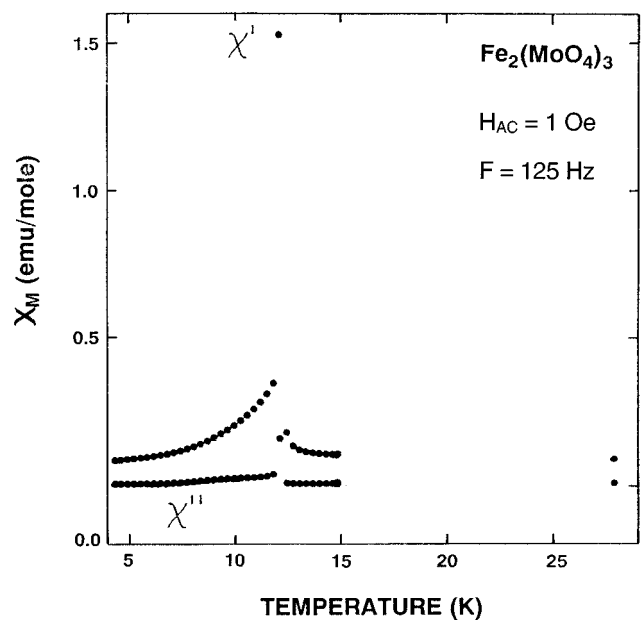


FIG. 6. Low-field ac susceptibility data for the precursor  $\text{Fe}_2(\text{MoO}_4)_3$  ( $H_0 = 1$  Oe, 125 Hz) showing a small, but clearly observed, out-of-phase signal,  $\chi''_m$ , characteristic of a ferromagnetic ground state.

signal,  $\chi''_m$ . For a perfectly collinear Néel antiferromagnet,  $\chi''_m = 0$ . Thus, canting and a net nonzero (weakly ferromagnetic) ground state are indicated. Previous studies (vibrating sample magnetometry and relatively high field ( $\sim 1$  to 5 Tesla) Faraday measurements) of the precursor-ferric material by Battle *et al.* (7) and Jirak *et al.* (8) indicate complex weak (so-called L-type) ferrimagnetism for  $\text{Fe}_2(\text{MoO}_4)_3$  with  $T_{\text{Néel}} \sim 13$  K. The present ac data of Fig. 6 are clearly consistent with the latter 3D ground state. We observe a small but definite imaginary component  $\chi''_m \neq 0$  at 13 K that accompanies the excursion in  $\chi'_m$ .

#### ACKNOWLEDGMENTS

We thank E. Prince for obtaining the neutron data, G. M. Wltschek and E. C. Rowlands for assistance in fitting the neutron data, and D. E. Cox for valuable discussions.

#### REFERENCES

1. W. M. Reiff, J. H. Zhang, and C. C. Torardi, *J. Solid State Chem.* **62**, 231 (1986).
2. C. C. Torardi and E. Prince, *Mater. Res. Bull.* **21**, 719 (1986).
3. C. C. Torardi, W. M. Reiff, J. H. Zhang, and E. Prince, *Mater. Sci. Forum* **27/28**, "Neutron Scattering Advances and Applications," p. 223. Trans Tech Publications, Switzerland (1988).
4. A. C. Larson, R. B. Von Dreele, Los Alamos Laboratory Rep. No. LA-UR-86-748, 1987.
5. E. F. Bertaut, in "Magnetism" (G. T. Rado and H. Suhl, Eds.), Vol. III. Academic Press, New York (1963).
6. J. P. Attfield, A. K. Cheetham, D. C. Johnson, and C. C. Torardi, *Inorg. Chem.* **26**, 3379 (1987).
7. P. D. Battle, A. K. Cheetham, G. J. Long, and G. Longworth, *Inorg. Chem.* **21**, 4223 (1982).
8. Z. Jirak, R. Salmon, L. Fournes, F. Menil, and P. Hagemuller, *Inorg. Chem.* **21**, 4218 (1982).